

This is an Open Access document downloaded from ORCA, Cardiff University's institutional repository: <https://orca.cardiff.ac.uk/id/eprint/100297/>

This is the author's version of a work that was submitted to / accepted for publication.

Citation for final published version:

Seema, Humaira, Shirinfar, Bahareh, Shi, Genggongwo, Youn, Il Seung and Ahmed, Nisar 2017. Facile synthesis of selective biomolecule chemosensor and fabrication of its highly fluorescent graphene complex. *Journal of Physical Chemistry B* 121 (19) , pp. 5007-5016. 10.1021/acs.jpcc.7b02888

Publishers page: <http://dx.doi.org/10.1021/acs.jpcc.7b02888>

Please note:

Changes made as a result of publishing processes such as copy-editing, formatting and page numbers may not be reflected in this version. For the definitive version of this publication, please refer to the published source. You are advised to consult the publisher's version if you wish to cite this paper.

This version is being made available in accordance with publisher policies. See <http://orca.cf.ac.uk/policies.html> for usage policies. Copyright and moral rights for publications made available in ORCA are retained by the copyright holders.



Facile Synthesis of Selective Biomolecule Chemosensor and Fabrication of Its Highly Fluorescent Graphene Complex

By Humaira Seema^{a,b*}, Bahareh Shirinfar^c, Genggongwo Shi^{a,d}, Il Seung Youn^{a,d} and Nisar Ahmed^{e*}

*E-mail: AhmedN14@cardiff.ac.uk, hawkkhan2@gmail.com

^a Department of Chemistry, Ulsan National Institute of Science and Technology (UNIST), Ulsan 689-798, Korea.

^b Institute of Chemical Sciences, University of Peshawar, KPK 25120, Pakistan

^c School of Chemistry, University of Bristol, Bristol, BS8 1TS, United Kingdom.

^d Department of Chemistry, Pohang University of Science and Technology, Pohang 790-784, Korea

^e School of Chemistry, Cardiff University, Main Building, Park Place, Cardiff, CF10 3AT, United Kingdom

ABSTRACT:

A novel hydrophilic imidazolium fluorescent chemosensor has been utilized to prepare water soluble fluorescent graphene complex via a facile ion exchange strategy, which gives a relatively very high quantum yield (0.87). The highly fluorescent graphene complex displays a close resemblance with the water soluble fluorescent chemosensor as the chemisorbed imidazolium hinders the electron transfer between the naphthalene moiety and the graphene. If the imidazolium is simply physisorbed on graphene by physical mixing, it does not show high quantum yield because the π - π stacking between the naphthalene moiety and graphene leads to fluorescence quenching. The fluorescent chemosensor selectively detects RNA by turn-on fluorescence at physiological pH in aqueous solution. The fluorescent chemosensor as well as the fluorescent graphene complex would yield potential applications as photoresponsive materials and biomedical probes.

INTRODUCTION

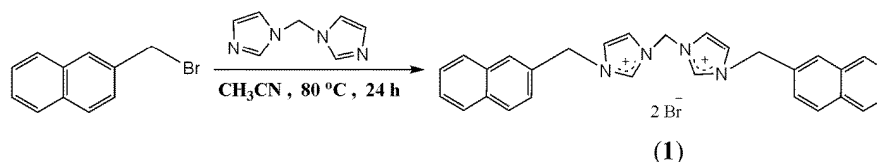
In recent times there has been a drastic increase of interest in graphene and functionalized graphene.¹⁻³ It is all due to its unique physicochemical properties with high surface area, strong mechanical strength, excellent electrical, thermal and optical properties,⁴ as well as its potential uses in electronics,⁵⁻⁶ energy materials,⁷⁻¹⁰ environmental remediation,¹¹⁻¹⁵ and bio-applications.¹⁶⁻²¹ Fluorescent graphene complexes have attracted more attention because of their promising nanoscale applications, while the photoluminescence properties of graphene complexes can be realized by functionalizing graphene with fluorescent materials²²⁻²⁶ through covalent or non-covalent interactions. Liu *et al.* described indicator displacement assay (IDA)-based fluorescence method for detection of heparin and protamines²⁷⁻²⁸ where fluorescent probe was used as an indicator. Upon addition of graphene based material the fluorescence of molecules on graphene via π - π stacking interaction is quenched due to the effective energy and electron transfer between them which leads to a challenge to prepare highly fluorescent graphene based material towards numerous applications.²⁹⁻³⁰ However, the target molecules (heparin or protamines) were selectively detected due to fluorescence turn on pathway. Liu *et al.* also prepared water dispersible functionalized graphene oxide (GO) nanocomposite and used for waste water remediation.³¹ Imidazolium based ionic liquids can interact with graphene to prepare stable dispersions in various matrices.³²⁻³³ Carbon nanotubes with imidazolium based salts via ion exchange showed stable dispersion and strong visible fluorescence.³⁴

Fluorescent probes have been widely used for biomolecular recognition, disease diagnosis and environmental pollution detection³⁵⁻³⁸ but still the detection of a specific bioanions by water soluble fluorescent molecule at physiological pH is challenging as there are a large number of important biomolecules in cells. Biomolecule detection through ionic hydrogen bonding is a challenging task in aqueous solution due to potential interference from the solvent. In the case of RNA and DNA, it is particularly more so due to the electronegative potentials. However, before functionalizing graphene with water soluble acyclic naphthimidazolium based

fluorescent probe **1**, we analyzed potential sensing application of **1** for biomolecules at physiological pH and observed selective turn-on fluorescence for RNA over other biomolecules. We anticipate that the present fluorescent probe could serve as a new tool in biological studies that aids in the future rational molecular and drug design by using simple cationic molecules directed to RNA. Naphthimidazolium salt **1** was synthesized in a simple one step reaction (Scheme 1) and further was attached to carboxyl functionalized graphene nanosheets to produce fluorescent graphene complex with high quantum yield via simple ion exchange strategy.

RESULTS AND DISCUSSION

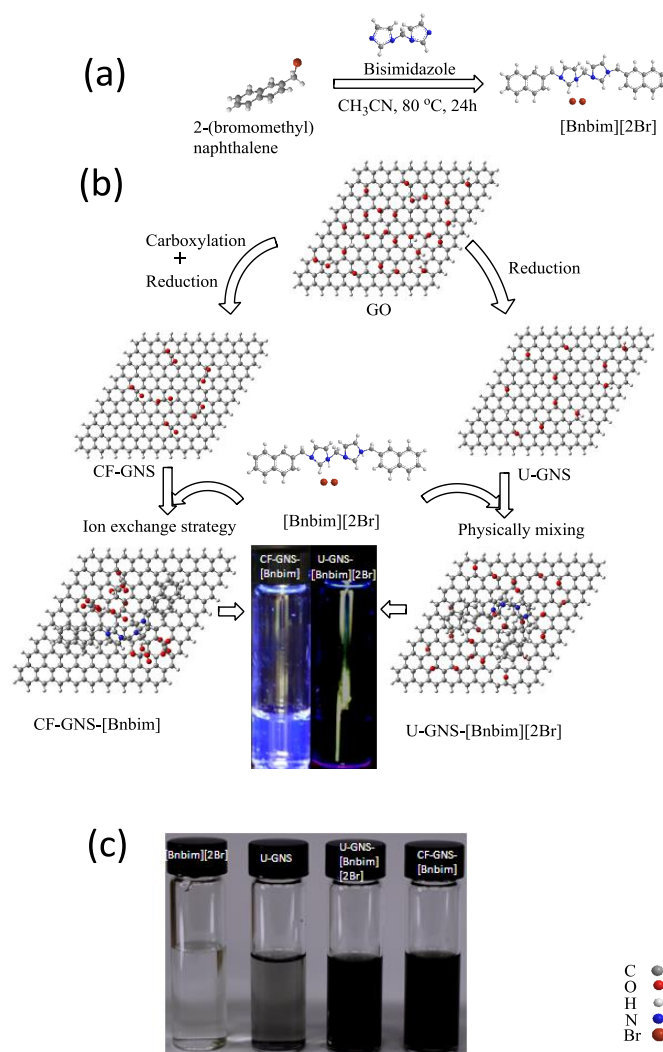
The fluorescent water soluble acyclic naphthimidazolium salt, 1,1'-methylene bis[3,3'-di(2-naphthylmethyl)imidazolium] dibromide, ([Bnbim][2Br]) was synthesized by the reaction of 2-(bromomethyl)naphthalene with 1-(1*H*-imidazol-1-ylmethyl)-1*H*imidazole in dried CH₃CN followed by recrystallization (ethanol) in 76% yield (Scheme 1).



Scheme 1. Synthesis of [Bnbim][2Br] (**1**)

The preparation of hydrophilic fluorescent graphene complex is illustrated in Scheme 2. The graphene oxide (GO) sheet as prepared by modified Hummer's method³⁹ contains a range of reactive oxygen functional groups, such as carboxylic acid groups at their edges while epoxy and hydroxyl groups on the basal planes.⁴⁰ To prepare carboxyl functionalized chemically converted graphene nanosheets (CF-GNS), the epoxy and hydroxyl groups of GO were converted to carboxylate groups,²¹ followed by reduction with glucose in aqueous ammonia.⁴¹ Unfunctionalized chemically converted graphene nanosheets (U-GNS) were also prepared by reduction method^{1,39} without carboxylation step. The aqueous solution of CF-GNS was reacted with aqueous fluorescent naphthimidazolium based salt [Bnbim][2Br] to prepare

aqueous stable dispersion of fluorescent graphene complex CF-GNS-[Bnbim] by ion-exchange strategy. The simultaneous formation of sodium bromide (NaBr) was removed by repeatedly washing with water and dialysis as shown in Scheme 2b. Moreover, polydispersibility in water and several organic solvents will make CF-GNS-[Bnbim] an ideal candidate for various applications.



Scheme 2 (a) Synthesis of [Bnbim][2Br] (**1**). (b) Synthesis of fluorescent graphene complex CF-GNS-[Bnbim] by ion-exchange strategy and synthesis of non-fluorescent graphene material U-GNS-[Bnbim][2Br] by physically grinding. (c) Photographs of aqueous solutions of [Bnbim][2Br], U-GNS, U-GNS-[Bnbim][2Br] and CF-GNS-[Bnbim] material (from left to right).

The unfunctionalized chemically converted graphene complex U-GNS-[Bnbim][2Br] was prepared as a control material by physically grinding the U-GNS with [Bnbim][2Br], followed by washing and dialysis to remove excess naphthimidazolium based salt (Scheme 2b).

X-ray diffraction (XRD) analysis (shown in Figure. 1) was carried out in order to investigate and compare the exfoliation of GO and CF-GNS-[Bnbim]. A characteristic strong and sharp peak observed for GO at $2\theta=11.8^\circ$ corresponds to an interlayer spacing of ~ 0.76 nm.⁴¹ The XRD analysis exhibits a diffraction peak of graphite at $2\theta=26.6^\circ$ which corresponds to an interlayer spacing of ~ 0.34 nm. However, it is worthwhile to note that no obvious peaks regarding graphite or GO could be found for CF-GNS-[Bnbim], indicative of the complete reduction and exfoliation to the CF-GNS-[Bnbim] which was successfully obtained in this work.⁴²

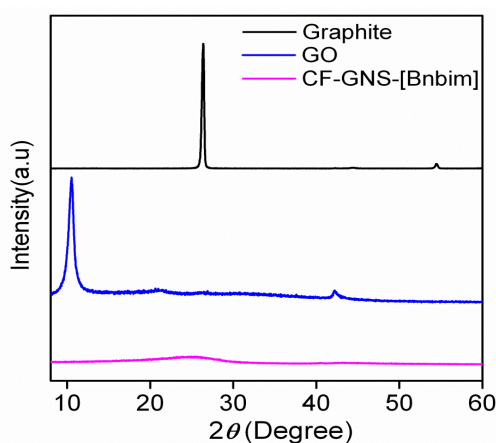


Figure 1. XRD of Graphite (black line), GO (blue line) and CF-GNS-[Bnbim] (pink line).

Fourier-transform infrared (FTIR) transmission spectra of CF-GNS and CF-GNS-[Bnbim] materials were recorded using KBr pellets (Figure 2). The FTIR spectrum of CF-GNS-[Bnbim] shows an absorption band at 2917 cm^{-1} due to C–H vibrations in the [Bnbim]²⁺ cation. The spectrum at 2851 cm^{-1} exhibits C–H...O hydrogen bonds between [Bnbim]²⁺ cation and CF-GNS material,^{43,44} which verifies that the [Bnbim]²⁺ cations are linked with the CF-GNS. The absorption bands at 1714 and 1060 cm^{-1} attributed to C=O and C–O bonds in the carboxylate groups, while that at 1562 cm^{-1} corresponds to the C=N bonds of imidazolium cation. The

broadening of the spectrum is possibly due to the overlap of C=N bond vibrations with that of C=C bond. The linkage of the CF-GNS to the [Bnbim]²⁺ cation modifies the C=N stretching displacement, in which the absorption band is red shifted to 1562 cm⁻¹ from 1571 cm⁻¹. The absorption band at 1175 cm⁻¹ corresponds to C-N bond and perhaps also overlaps with the vibration band of the GNS at 1155 cm⁻¹.

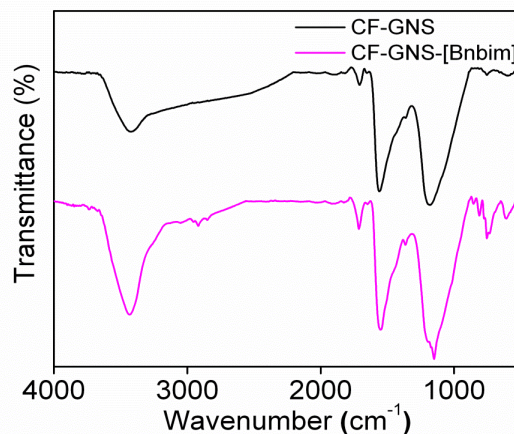


Figure 2. FT-IR spectra of CF-GNS (black line) and CF-GNS-[Bnbim] (pink line).

To investigate further the interaction between [Bnbim]²⁺ cation and CF-GNS, the resulting CF-GNS and CF-GNS-[Bnbim] materials were characterized by Raman spectroscopy. The Raman spectra of the CF-GNS and CF-GNS-[Bnbim] (Figure 3) illustrate broad peaks that correspond to the D band at 1308 and 1322 cm⁻¹, respectively, and the G band at 1592 and 1606 cm⁻¹, respectively. These peaks are significantly shifted by 14 cm⁻¹ in the CF-GNS-[Bnbim] material as compared to those in CF-GNS, most likely due to charge-transfer between the CF-GNS and [Bnbim]²⁺ cation, which provides further evidence²⁺ for the formation of the CF-GNS-[Bnbim] material. In addition, compared to CF-GNS, the decrease in intensity ratio of D/G for the CF-GNS-[Bnbim] material indicates that the functionalization of CF-GNS with the [Bnbim]²⁺ cation increases the G band intensity of the graphene sheets.⁴⁵

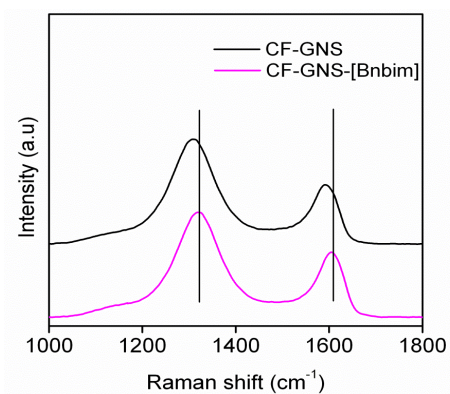


Figure 3. Raman spectra of CF-GNS (black line) and CF-GNS-[Bnbim] (pink line).

Figure 4 shows atomic force microscopy (AFM) analysis of CF-GNS and CF-GNS-[Bnbim]. The single-layered CF-GNS with a thickness of about 0.71 nm has a relatively smooth surface,^{46,47} whereas the attachment of the [Bnbim]²⁺ cations results in much rougher surface of CF-GNS-[Bnbim] sheets. AFM analysis depicted that the thickness of the [Bnbim] layer is ~ 0.82 nm, which is almost similar to the thickness of surfactant adsorbed on the surface of graphene.⁴⁸ The AFM image of U-GNS shows thickness of ~ 0.70 nm (Supporting Information S3).

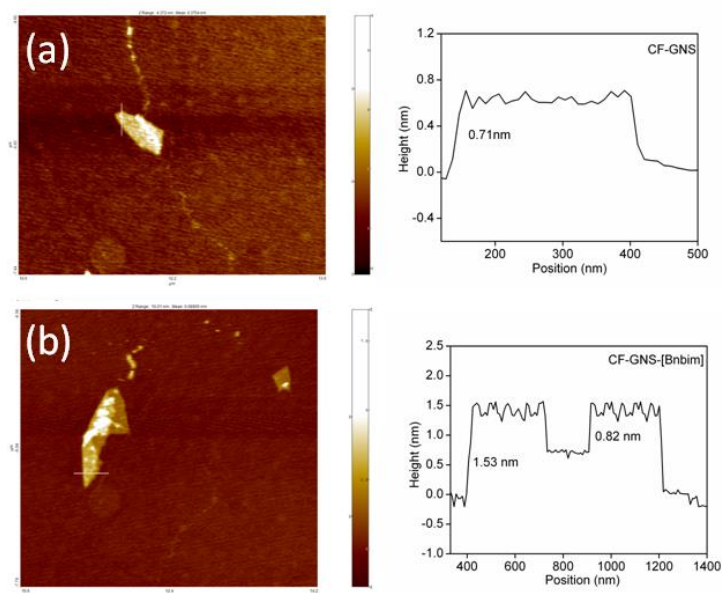


Figure 4. AFM images of (a) CF-GNS and (b) CF-GNS-[Bnbim] with their respective height profiles.

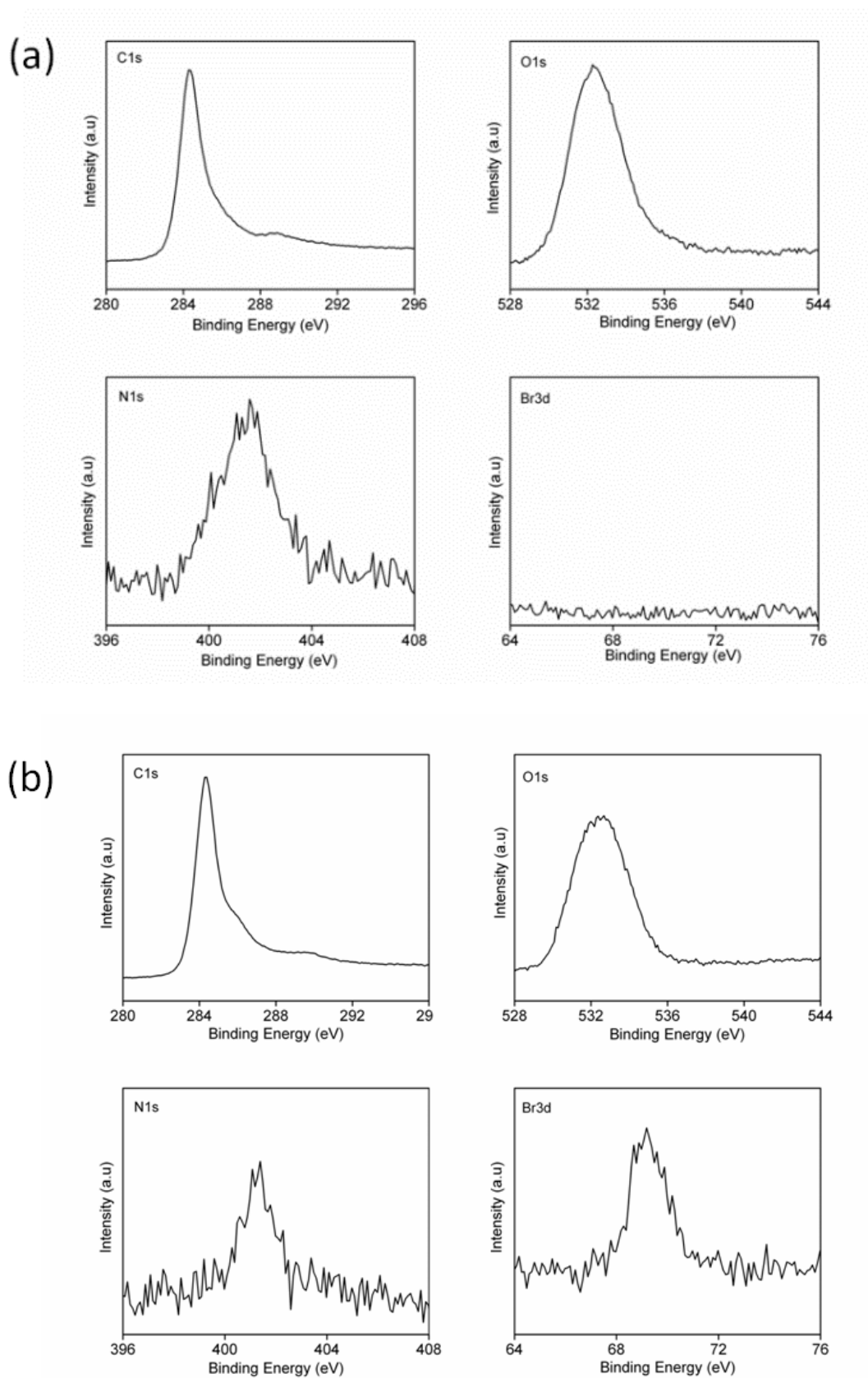


Figure 5. XPS survey scans of (a) CF-GNS-[Bnbim] and (b) U-GNS-[Bnbim][2Br].

X-ray photoelectron spectroscopy (XPS) analysis confirms the exchange of the sodium ions in the CF-GNS by the [Bnbim]²⁺ cation via ion exchange strategy (Figure 5a). The XPS spectra of CF-GNS shows a peak corresponding to sodium, which is absent in XPS analysis of the CF-GNS-[Bnbim] (Supporting Information S4). This indicates that sodium cations have been removed from CF-GNS as NaBr, which confirms the ion exchange process. The survey of the XPS analysis of the CF-GNS-[Bnbim] material does not show peaks corresponding to bromide (Br 3d, 69.1 eV), indicating that the bromide anion in the [Bnbim][2Br] precursor has been removed as NaBr, while it illustrates the peak of nitride (N1s, 401.2 eV).³⁴ In contrast, the XPS analysis of the U-GNS-[Bnbim][2Br] sample displays the presence of bromide and nitride (Figure 5b).

Transmission electronic microscopy (TEM) was used to characterize the morphology of the CF-GNS-[Bnbim] material. Figure 6 shows graphene sheets with some overlapping,⁴⁹ while the corresponding selected-area electron diffraction (SAED) pattern displays a typical six-fold symmetry diffraction patterns, which is assigned to graphene (inset in Figure 6).^{50,51}

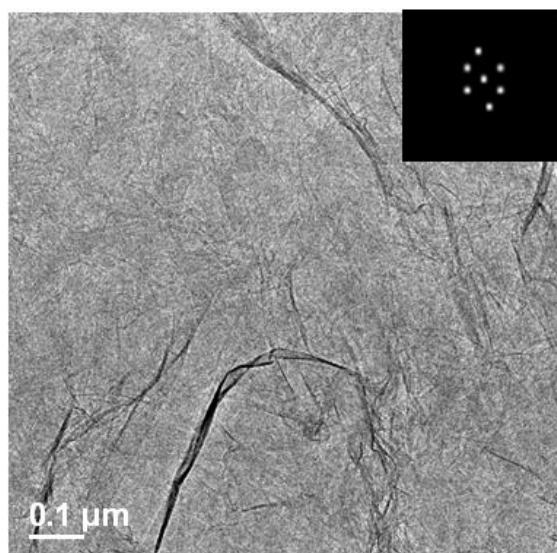


Figure 6. TEM image of CF-GNS-[Bnbim] and its SAED pattern (Inset).

The UV-Vis absorption spectrum of the U-GNS-[Bnbim][2Br] material is broader compared to those of [Bnbim][2Br] and CF-GNS-[Bnbim] (Figure 7). The spectra of both CF-GNS-

[Bnbim] and U-GNS-[Bnbim][2Br] show a peak at 265 nm, which corresponds to graphene. The broadening in the spectrum of U-GNS-[Bnbim][2Br] reveals π - π interactions⁵² between the naphthalene ring plane in the [Bnbim]²⁺ cation and the surface of U-GNS, which are prevented to a greater extent in the CF-GNS-[Bnbim] material. Due to similar spectral shape in UV/Vis spectroscopic analysis it is possible to suggest that the [Bnbim]²⁺ cation in the ionic CF-GNS-[Bnbim] composite adopts the same electronic structure as that in the naphthimidazolium salt [Bnbim][2Br].

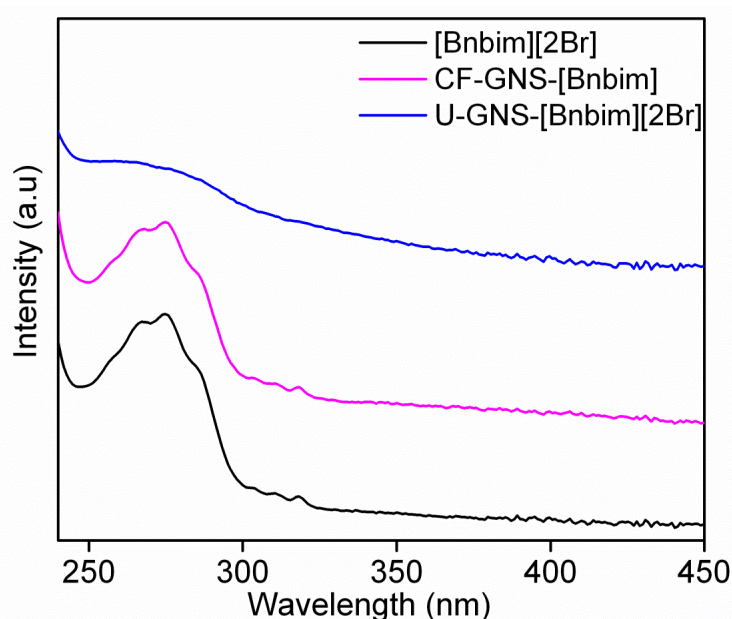


Figure 7. UV/visible absorption spectra of [Bnbim][2Br] (black line), CF-GNS-[Bnbim] (pink line) and U-GNS-[Bnbim][2Br] (blue line). ([Bnbim]²⁺ = 10 μ M in all samples).

To compare the fluorescence behavior of [Bnbim][2Br], U-GNS-[Bnbim][2Br] and CF-GNS-[Bnbim] materials, the photoluminescence spectra were measured (Figure 8). Similar but somewhat weaker emission peaks are observed for CF-GNS-[Bnbim] material compared to [Bnbim][2Br], while U-GNS-[Bnbim][2Br] does not show any fluorescence even at a series of concentrations. The [Bnbim]²⁺ cation interacts with the graphene surfaces predominantly through electrostatic interactions which lead to high fluorescence of the ionic CF-GNS-[Bnbim]. In addition, most naphthalene moieties are prevented from interacting with the sheet

due to the carboxyl groups protruded from the graphene sheet (Figure 9a). Simultaneously there is another possibility that some naphthalene moieties interact with the sheet through π - π interaction (Figure 9). The proportion of those π - π interactions is, however, small compared to the total number of the fluorescent probes, and thus the fluorescence peak shows only small reduction, instead of the complete quenching. On the other hand, the quenching of the fluorescence of [Bnbim][2Br] in U-GNS-[Bnbim][2Br] material suggests π - π stacking (Figure 10) which is indicative of electronic communication between the π -systems of U-GNS and the [Bnbim][2Br]. The linkage in CF-GNS-[Bnbim] connecting the naphthalene rings to CF-GNS efficiently prevents electron transfer from naphthalene in excited state to CF-GNS. As a consequence, it maintains the electronic states of [Bnbim][2Br] to a greater extent, which is in accordance with the result of fluorescence emission and UV absorption spectra.²³⁻²⁶

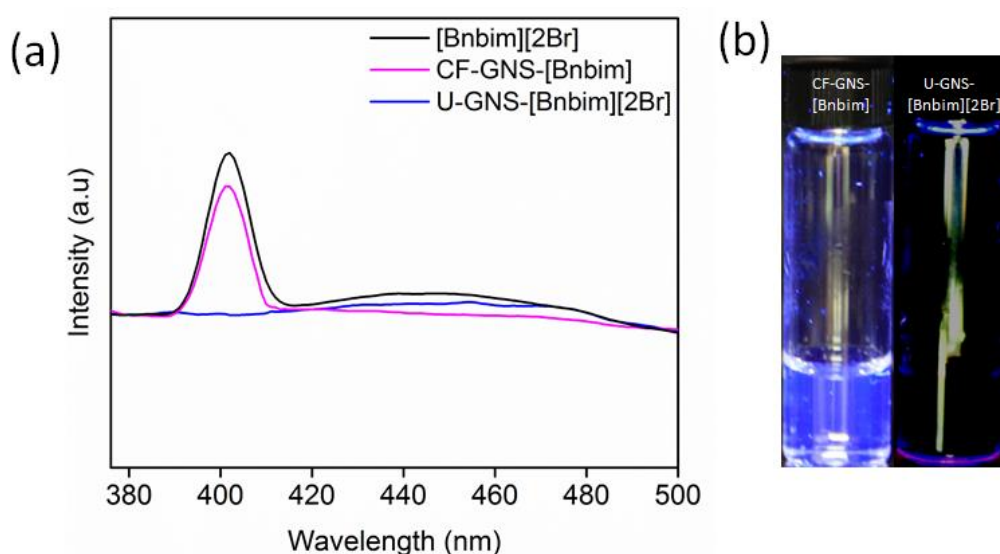


Figure 8. Fluorescence emission spectra of [Bnbim][2Br] (black line), CF-GNS-[Bnbim] (pink line) and U-GNS-[Bnbim][2Br] (blue line) (a), while the fluorescence images of CF-GNS-[Bnbim] (left) and U-GNS-[Bnbim][2Br] (right) (b). ($[Bnbim]^{2+} = 10\mu M$ in all samples).

The difference in fluorescence of materials can be evaluated from their relative quantum yields (Φ). The concentration independent value of Φ at the steady-state was measured as [Bnbim][2Br] (1.00) > CF-GNS-[Bnbim] ($\Phi = 0.87$) > U-GNS-[Bnbim][2Br] (Φ is negligible)

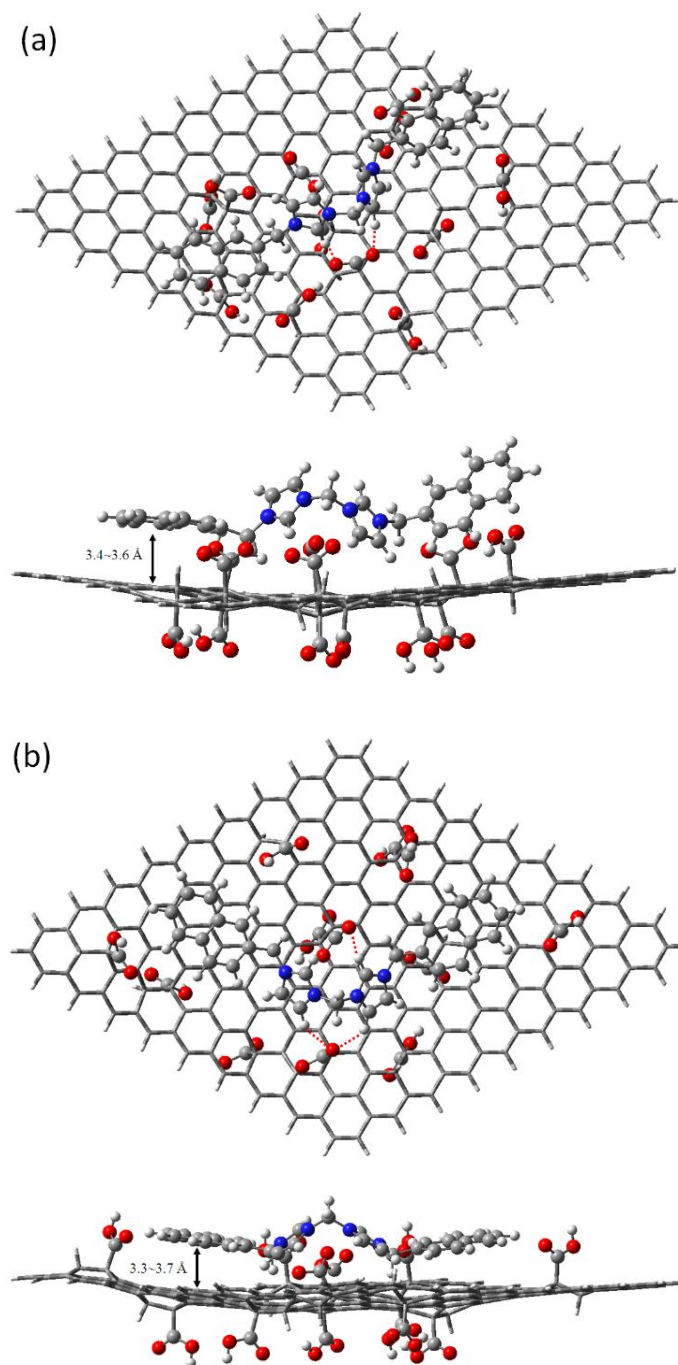


Figure 9. Top and side views of two optimized structures (a, b) of CF-GNS with naphthimidazolium probe **1** [Bnbim][2Br]. The graphene sheet is represented as tube model, while probe **1** and carboxyl groups are depicted as ball-and-stick model. The ionic interactions between the naphthalene moieties and carboxylates are indicated by red dotted lines. (Red: oxygen; crimson red: grey: carbon; white: hydrogen; blue: nitrogen).

whereas by using naphthalene as a standard, Φ of [Bnbim][2Br] and CF-GNS-[Bnbim] are 0.86 and 0.53 respectively in ethanol.³⁴ Some π - π interactions between the naphthalene rings and the graphene sheets are probable to exist, and graphene can absorb or scatter the excitation light which results in a decrease of the quantum yield of CF-GNS-[Bnbim].

Fluorescence titrations were carried out in aqueous solution at pH 7.4 (10 mM phosphate buffer). Figure 10a shows visual features, while Figure 10b displays the fluorescence emission changes in naphthimidazolium probe **1** [Bnbim][2Br] in the presence of 1 equivalent of DNA, RNA, glucose, heme, TBA salts of F^- , Cl^- , NO_3^- and sodium salts of phosphate anions (ATP, GTP, CTP, TTP, UTP, pyrophosphate (PPi)). As shown in Figure 10b, there was unique change in the emission spectrum upon addition of RNA. The blue color enhancement of the **1**-RNA solution (Figure 10b) can be attributed to turn-on fluorescence in the emission spectrum due to formation of more stable complex with RNA, while it displays no particular response to other bioanions.⁵³ The enhancement of fluorescence with increasing concentration (0 to 5 equivalents) of RNA was noted (Figure Figure 10c, d. The most important driving force for the increase in fluorescence in the presence of RNA could be ascribed to the electrostatic interaction of the positively charged probe **1** with the phosphate and hydroxyl groups of RNA. In addition, π -stacking of the aromatic part of probe **1** in the major groove region of RNA, allows turn-on selective detection of RNA, while it displays no particular response to other bioanions. Positively charged molecules interact with the electronegative region of RNA/DNA. Therefore noncovalent interactions for RNA fluorescence sensing by positively charged molecules would be governed by the more electronegative potential on the surface of the RNA major groove, besides shape complement to the major groove of RNA.

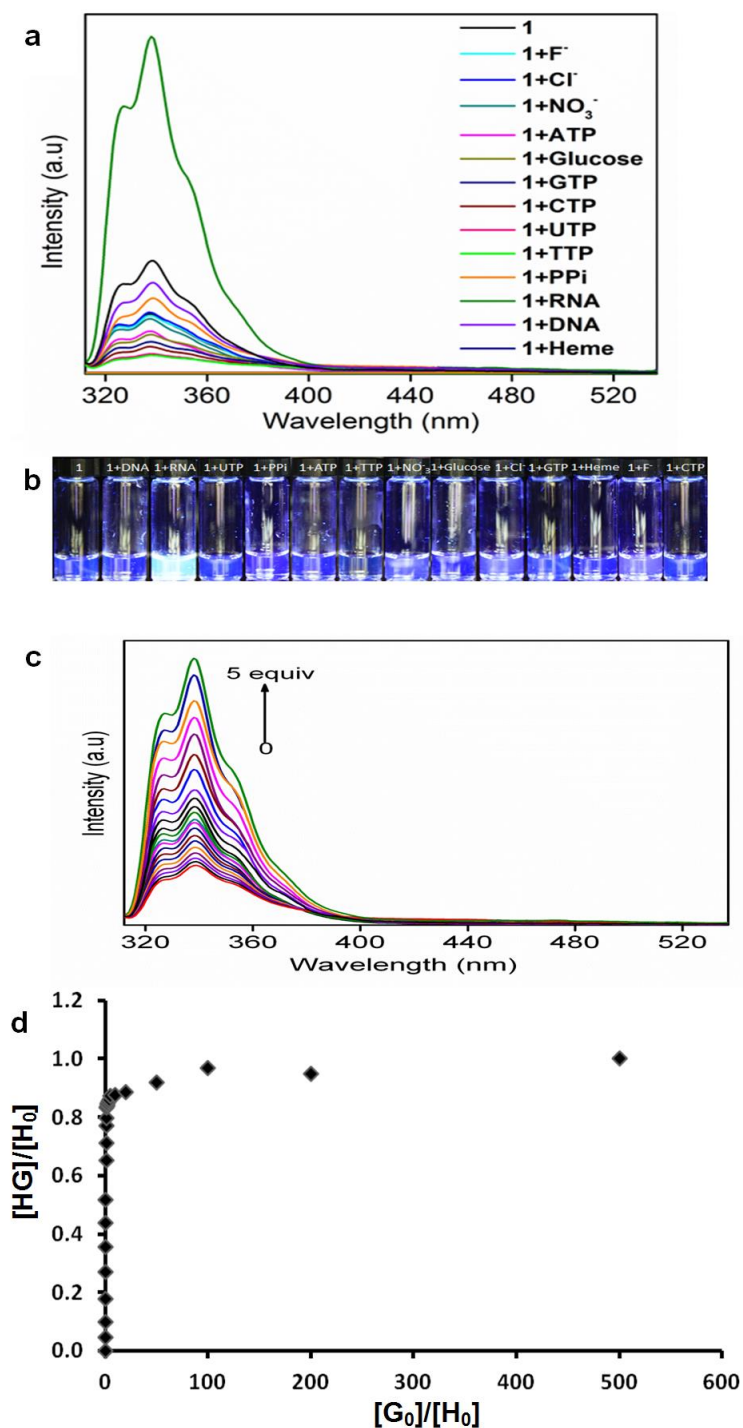


Figure 10. (a) Fluorescence (slit width = 5 nm; excitation at 274nm) of [Bnbim][2Br] **1** (10 μM) upon addition of DNA, RNA, glucose, heme, TBA salts of F⁻, Cl⁻, NO₃⁻ and sodium salts of ATP,GTP, CTP, TTP, UTP, PPi, (1 equiv each) at pH 7.4 (10 mM phosphate buffer) and (b) the corresponding visual fluorescence features. (c, d) Emission spectra (slit width = 5 nm; excitation at 274nm) of [Bnbim][2Br] **1** (10 μM) upon addition of sodium salt of RNA at pH 7.4 (10 mM phosphate buffer).

COMPUTATIONAL RESULTS

The computational results show that the imidazolium moieties of probe **1** are captured by two Br⁻ with ionic interaction at a distance of 2.3~2.4 Å. The naphthalene moieties interact with a U-GNS sheet through π - π interaction at a distance of about 3.2~3.5 Å (Figure 11). On the other hand, probe **1** is captured by carboxyl groups on the CF-GNS through ionic interaction at a distance of 1.8~2.6 Å. Besides the ionic interaction between imidazolium moieties and carboxylic oxygen atoms, there is also π - π interaction between naphthalene moieties and CF-GNS sheet at a distance of 3.3~3.6 Å (Figure 9a) or 3.3~3.7 Å (Figure 9b).

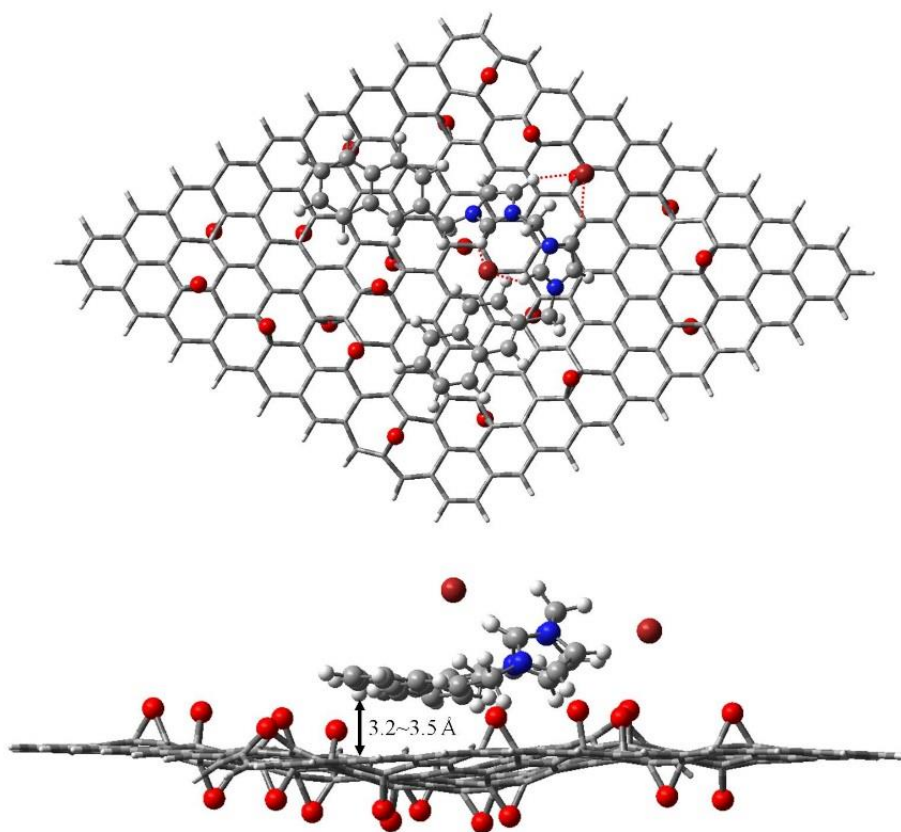


Figure 11. Top and side views of the optimized structure of U-GNS with probe **1**. The graphene sheet is represented as tube model, while the probe **1**, Br⁻ and ether groups are depicted as ball-and-stick model. The ionic interactions between the naphthalene moieties and two Br⁻ are indicated by red dotted lines. (Red: oxygen; grey: carbon; white: hydrogen; blue: nitrogen).

EXPERIMENTAL SECTION

Materials: Graphite (325 mesh, Alfa Aesar), hydrogen peroxide (30% wt, Aldrich), sulphuric acid, hydrochloric acid, hydrazine (80%, Aldrich), glucose (Aldrich), 2-(bromomethyl)naphthalene (Aldrich), imidazole (Aldrich), acetonitrile (Aldrich), ethanol (Aldrich). Sodium salts of pyrophosphate (PPi), ATP, GTP, CTP, TTP, UTP, hemoglobin from bovine blood cells (heme), Ribonucleic acid, transfer from baker's yeast (*S-cerevisiae*), DNA from calf thymus (CT DNA) and n-TBA salts of F⁻ and Cl⁻ were purchased from Aldrich and used for titrations without further purification.

Characterization and Instrumentation: X-ray diffraction patterns (XRD) were carried out using a Riguka, Japan, RINT 2500 V X-ray diffraction-meter with Cu K α irradiation ($\lambda = 1.5406 \text{ \AA}$). Fourier transformed infrared (FTIR) spectra were measured in KBr pellets with a Bruker FTIR. Raman spectra were recorded using a Senterra Raman Scope system with a 532nm wavelength incident laser light and power 20 mW. Transmission electron microscopy (TEM) and high-resolution transmission electron microscopy (HRTEM) observations were performed on a JEM-2100F (Cs corrected STEM) electron microscope with an accelerating voltage of 200 kV. XPS analysis was carried out with an ESCALAB-220I-XL (THERMO-ELECTRON, VG Company) device. Photoemission was stimulated by a nonmonochromatized Mg K α source (1253.6 eV) for all samples. Absorption (UV-Vis) spectra were recorded at room temperature using a Shanghi 756 MC UV-Vis spectrophotometer. Fluorescence spectra were measured at room temperature on Shimadzu RF-5301 PC spectrofluorophotometer. ¹H NMR and ¹³C NMR spectra were performed on a Bruker Advance DPX500 (500 MHz) spectrometer at 298 K.

Preparation of [Bnbim][2Br] (I): 1-(1H-imidazol-1-ylmethyl)-1Himidazole (1 mmol, 148mg) and 2-(bromomethyl) naphthalene (1 mmol, 221mg) were dissolved in dried CH₃CN (50mL) and were refluxed at 80°C for 24 hours. The resulting hot solution was filtered and the obtained white solid product was washed with CH₃CN and then crystallized from ethanol. Afterwards,

the white product, [Bnbim][2Br], dried under vacuum oven and the precipitated solid product gave 76 % yield in this experiment. The resulting compound was characterized by NMR spectroscopy (^1H NMR and ^{13}C NMR) which confirmed the structure of probe (**1**) as shown in Supporting Information S1 and S2. ^1H NMR (500MHz, D_2O , δ): 7.97-7.94 (m, 8H, -CH=), 7.80 (s, 2H, -CH=), 7.69 (s, 2H, -CH=), 7.64 (s, 4H, -CH=), 7.48-7.46 (s, 2H, -CH=), 6.69 (s, 2H, -CH₂-), 5.63 (s, 4H, -CH₂-). ^{13}C NMR (500MHz, D_2O , δ): 130.1, 129.3, 128.5, 128.0, 127.8, 127.4, 127.1, 125.5, 123.9, 122.2, 59.0, 53.6. Anal. Calcd for $\text{C}_{29}\text{H}_{26}\text{Br}_2\text{N}_4$: C 59.00, H 4.44, N 9.49; found: C 57.56, H 4.342, N 9.106.

Preparation of CF-GNS: Carboxylated graphene nanosheets solution (CF-GNS) was prepared by a modified literature procedure.²¹ First of all, GO (1mg mL^{-1}) solution was prepared in 100 mL distilled water using sonicator. NaOH (5 g) and ClCH₂COOH (5 g) were added to the GO suspension and sonicated for 1-2h resulting in carboxylated functionalized graphene nanosheets solution which was purified by repeated washing and collected by filtration. 10mL of 2% Na₂CO₃ was added to 100mL aqueous solution of the obtained solid and the mixture was sonicated for a while. The resulting solution was neutralized by repeated washing and centrifugation. The obtained solid was dispersed in distilled water (100mL) after that glucose (250 mg) and ammonia solution (100 μL , 25% w/w) were added. The mixture was stirred for 5 h at 85⁰C after vigorously stirring at room temperature. The final product was obtained by centrifugation, rinsed with water (25 mL) three times and then vacuum dried.

Preparation of U-GNS: Graphene oxide (GO) was synthesized by a modified Hummers method.⁴⁴ Unfunctionalized graphene nanosheets solid was obtained by the hydrazine reduction of the as obtained graphene oxide.⁵⁴

Preparation of CF-GNS-[Bnbim]: 200mL aqueous solution of CF-GNS (100 mg) was added to 100mL aqueous solution of [Bnbim][2Br] (3×10^{-3} M), and sonicated for 2 h then the mixture

was heated in the dark for 12 h at 80 °C. The solid product was obtained after filtration, washed repeatedly with ethanol and water, and then purified by dialysis.

Preparation of U-GNS-[Bnbim][2Br]: 100mg U-GNS was ground with 5 mg of [Bnbim][2Br] for 1 h during which water (10 mL) was added drop wise. The mixture was centrifuged after ultrasonication for 5 h. The obtained material was filtered and washed with ethanol and water, and then purified by dialysis.

CONCLUSIONS

We designed a acyclicwater soluble fluorescent probe which not only shows selective turn-on fluorescence for RNA butalso produced fluorescent graphene complex via ion exchange strategy. The fluorescent graphene complex with relatively high quantum yield (0.87) displays a close resemblance in the electronic state of water soluble fluorescent [Bnbim]²⁺ cation. The fluorescent graphene complex may find potential applications as photoresponsive materials and biomedical probes.

Supporting Information

The Supporting Information is available free of charge on the ACS Publications website at <http://pubs.acs.org>.

ACKNOWLEDGEMENTS

Marie Skłodowska-Curie Actions COFUND Fellowship to Dr. Nisar. Ahmed is gratefully acknowledged. Newton Postdoctoral Fellowship to Dr. Bahareh shirinfar is acknowledged as well. The authors want to thank Prof. Kwang S. Kim (Department of Chemistry, Ulsan National Institute of Science and Technology (UNIST), Republic of Korea) for his continuous support.

REFERENCES

1. Zhu, Y.; Murali, S.; Cai, W.; Li, X.; Suk, J. W.; Potts, J. R.; Ruoff, R. S. Graphene and graphene oxide: synthesis, properties, and applications. *Adv. Mater.* **2010**, 22 (35), 3906-3924.

2. Georgakilas, V.; Otyepka, M.; Bourlinos, A. B.; Chandra, V.; Kim, N.; Kemp, K. C.; Hobza, P.; Zboril, R.; Kim, K. S. Functionalization of graphene: covalent and non-covalent approaches, derivatives and applications. *Chem. Rev.* **2012**, *112* (11), 6156-6214.
3. Loh, K. P.; Bao, Q.; Ang, P. K.; Yang, J. The chemistry of graphene. *J. Mater. Chem.* **2010**, *20* (12), 2277-2289.
4. Meyer, J. C.; Geim, A. K.; Katsnelson, M. I.; Novoselov, K. S.; Booth, T. J.; Roth, S. The structure of suspended graphene sheets. *Nature* **2007**, *446* (7131), 60-63.
5. Park, J.; Lee, W. H.; Huh, S.; Sim, S. H.; Kim, S. B.; Cho, K.; Hong, B. H.; Kim, K. S. Work-function engineering of graphene electrodes by self-assembled monolayers for high-performance organic field-effect transistors. *J. Phys. Chem. Lett.* **2011**, *2* (8), 841-845.
6. Lee, W. H.; Park, J.; Sim, S. H.; Jo, S. B.; Kim, K. S.; Hong, B. H.; Cho, K. Transparent flexible organic transistors based on monolayer graphene electrodes on plastic. *Adv. Mater.* **2011**, *23* (15), 1752-1756.
7. Zhu, Y.; Murali, S.; Stoller, M. D.; Ganesh, K.; Cai, W.; Ferreira, P. J.; Pirkle, A.; Wallace, R. M.; Cychosz, K. A.; Thommes, M. Carbon-based supercapacitors produced by activation of graphene. *Science* **2011**, *332* (6037), 1537-1541.
8. Wang, D.; Choi, D.; Li, J.; Yang, Z.; Nie, Z.; Kou, R.; Hu, D.; Wang, C.; Saraf, L. V.; Zhang, J. Self-assembled TiO₂-graphene hybrid nanostructures for enhanced Li-ion insertion. *ACS nano* **2009**, *3* (4), 907-914.
9. Tiwari, J. N. N., K.; Kumar, S.; Tiwari, R. N.; Kemp, K. C.; Le, N. H.; Youn, D. H.; Lee, J. S.; Kim, K. S. Stable platinum nanoclusters on genomic DNA-graphene oxide with a high oxygen reduction reaction activity *Nat. Commun.* **2013**, *4*.
10. Wang, X.; Zhi, L.; Tsao, N.; Tomović, Ž.; Li, J.; Müllen, K. Transparent carbon films as electrodes in organic solar cells. *Angew. Chem. Int. Ed.* **2008**, *120* (16), 3032-3034.
11. Liao, G.; Chen, S.; Quan, X.; Yu, H.; Zhao, H. Graphene oxide modified gC₃N₄ hybrid with enhanced photocatalytic capability under visible light irradiation. *J. Mater. Chem.* **2012**, *22* (6), 2721-2726.
12. Kemp, K. C.; Seema, H.; Saleh, M.; Le, N. H.; Mahesh, K.; Chandra, V.; Kim, K. S. Environmental applications using graphene composites: water remediation and gas adsorption. *Nanoscale* **2013**, *5* (8), 3149-3171.
13. Chandra, V.; Park, J.; Chun, Y.; Lee, J. W.; Hwang, I.-C.; Kim, K. S. Water-dispersible magnetite-reduced graphene oxide composites for arsenic removal. *ACS nano* **2010**, *4* (7), 3979-3986.
14. Myung, S.; Solanki, A.; Kim, C.; Park, J.; Kim, K. S.; Lee, K. B. Graphene - encapsulated nanoparticle - based biosensor for the selective detection of cancer biomarkers. *Adv. Mater.* **2011**, *23* (19), 2221-2225.
15. Park, S. Y.; Park, J.; Sim, S. H.; Sung, M. G.; Kim, K. S.; Hong, B. H.; Hong, S. Enhanced differentiation of human neural stem cells into neurons on graphene. *Adv. Mater.* **2011**, *23* (36).
16. Myung, S.; Yin, P. T.; Kim, C.; Park, J.; Solanki, A.; Reyes, P. I.; Lu, Y.; Kim, K. S.; Lee, K. B. Label - Free Polypeptide - Based Enzyme Detection Using a Graphene - Nanoparticle Hybrid Sensor. *Adv. Mater.* **2012**, *24* (45), 6081-6087.
17. Min, S. K.; Kim, W. Y.; Cho, Y.; Kim, K. S. Fast DNA sequencing with a graphene-based nanochannel device. *Nat. Nanotechnol.* **2011**, *6* (3), 162-165.
18. Shen, J.; Zhu, Y.; Yang, X.; Li, C. Graphene quantum dots: emergent nanolights for bioimaging, sensors, catalysis and photovoltaic devices. *Chem. Commun.* **2012**, *48* (31), 3686-3699.

19. Lee, W. C.; Lim, C. H. Y.; Shi, H.; Tang, L. A.; Wang, Y.; Lim, C. T.; Loh, K. P. Origin of enhanced stem cell growth and differentiation on graphene and graphene oxide. *ACS nano* **2011**, *5* (9), 7334-7341.
20. Zhang, X.; Yin, J.; Peng, C.; Hu, W.; Zhu, Z.; Li, W.; Fan, C.; Huang, Q. Distribution and biocompatibility studies of graphene oxide in mice after intravenous administration. *carbon* **2011**, *49* (3), 986-995.
21. Sun, X.; Liu, Z.; Welsher, K.; Robinson, J. T.; Goodwin, A.; Zaric, S.; Dai, H. Nano-graphene oxide for cellular imaging and drug delivery. *Nano. Res.* **2008**, *1* (3), 203-212.
22. Eda, G.; Lin, Y. Y.; Mattevi, C.; Yamaguchi, H.; Chen, H. A.; Chen, I.; Chen, C. W.; Chhowalla, M. Blue photoluminescence from chemically derived graphene oxide. *Adv. Mater.* **2010**, *22* (4), 505-509.
23. Lee, D.-W.; Kim, T.; Lee, M. An amphiphilic pyrene sheet for selective functionalization of graphene. *Chem. Commun.* **2011**, *47* (29), 8259-8261.
24. Kim, Y. T.; Han, J. H.; Hong, B. H.; Kwon, Y. U. Electrochemical Synthesis of CdSe Quantum - Dot Arrays on a Graphene Basal Plane Using Mesoporous Silica Thin - Film Templates. *Adv. Mater.* **2010**, *22* (4), 515-518.
25. Wang, Y.; Kurunthu, D.; Scott, G. W.; Bardeen, C. J. Fluorescence quenching in conjugated polymers blended with reduced graphitic oxide. *J. Phys. Chem. C* **2010**, *114* (9), 4153-4159.
26. Karousis, N.; Sandanayaka, A. S.; Hasobe, T.; Economopoulos, S. P.; Sarantopoulou, E.; Tagmatarchis, N. Graphene oxide with covalently linked porphyrin antennae: Synthesis, characterization and photophysical properties. *J. Mater. Chem.* **2011**, *21* (1), 109-117.
27. Liu, J.; Liu, G.; Liu, W.; Wang, Y. Turn-on fluorescence sensor for the detection of heparin based on rhodamine B-modified polyethyleneimine-graphene oxide complex. *Biosens. Bioelectron.* **2015**, *64*, 300-305.
28. Liu, J.; Xu, M.; Wang, B.; Zhou, Z.; Wang, L. Fluorescence sensor for detecting protamines based on competitive interactions of polyacrylic acid modified with sodium 4-amino-1-naphthalenesulfonate with protamines and aminated graphene oxide. *RSC Adv.* **2017**, *7* (3), 1432-1438.
29. Wang, Y.; Yao, H.-B.; Wang, X.-H.; Yu, S.-H. One-pot facile decoration of CdSe quantum dots on graphene nanosheets: novel graphene-CdSe nanocomposites with tunable fluorescent properties. *J. Mater. Chem.* **2011**, *21* (2), 562-566.
30. Cao, Y.; Yang, T.; Feng, J.; Wu, P. Decoration of graphene oxide sheets with luminescent rare-earth complexes. *Carbon.* **2011**, *49* (4), 1502-1504.
31. Liu, J.; Liu, G.; Liu, W. Preparation of water-soluble β -cyclodextrin/poly (acrylic acid)/graphene oxide nanocomposites as new adsorbents to remove cationic dyes from aqueous solutions. *Chem. Eng. J.* **2014**, *257*, 299-308.
32. Zhang, B.; Ning, W.; Zhang, J.; Qiao, X.; Zhang, J.; He, J.; Liu, C.-Y. Stable dispersions of reduced graphene oxide in ionic liquids. *J. Mater. Chem.* **2010**, *20* (26), 5401-5403.
33. Yang, H.; Shan, C.; Li, F.; Han, D.; Zhang, Q.; Niu, L. Covalent functionalization of polydisperse chemically-converted graphene sheets with amine-terminated ionic liquid. *Chem. Commun.* **2009**, (26), 3880-3882.
34. Fu, C.; Meng, L.; Lu, Q.; Fei, Z.; Dyson, P. J. A facile strategy for preparation of fluorescent SWNT complexes with high quantum yields based on ion exchange. *Adv. Funct. Mater.* **2008**, *18* (6), 857-864.
35. Shirinfar, B.; Ahmed, N.; Park, Y. S.; Cho, G.-S.; Youn, I. S.; Han, J.-K.; Nam, H. G.; Kim, K. S. Selective fluorescent detection of RNA in living cells by using imidazolium-based cyclophane. *JACS* **2012**, *135* (1), 90-93.

36. Xu, Z.; Singh, N. J.; Lim, J.; Pan, J.; Kim, H. N.; Park, S.; Kim, K. S.; Yoon, J. Unique sandwich stacking of pyrene-adenine-pyrene for selective and ratiometric fluorescent sensing of ATP at physiological pH. *JACS* **2009**, *131* (42), 15528-15533.
37. Kim, H. N.; Lee, E.-H.; Xu, Z.; Kim, H.-E.; Lee, H.-S.; Lee, J.-H.; Yoon, J. A pyrene-imidazolium derivative that selectively Recognizes G-Quadruplex DNA. *Biomaterials* **2012**, *33* (7), 2282-2288.
38. Rhee, H.-W.; Choi, H.-Y.; Han, K.; Hong, J.-I. Selective fluorescent detection of flavin adenine dinucleotide in human eosinophils by using bis (Zn²⁺-dipicolylamine) complex. *JACS* **2007**, *129* (15), 4524-4525.
39. Xu, Y.; Bai, H.; Lu, G.; Li, C.; Shi, G. Flexible graphene films via the filtration of water-soluble noncovalent functionalized graphene sheets. *JACS* **2008**, *130* (18), 5856-5857.
40. Dreyer, D. R.; Park, S.; Bielawski, C. W.; Ruoff, R. S. The chemistry of graphene oxide. *Chem. Soc. Rev.* **2010**, *39* (1), 228-240.
41. Zhu, C.; Guo, S.; Fang, Y.; Dong, S. Reducing sugar: new functional molecules for the green synthesis of graphene nanosheets. *ACS nano* **2010**, *4* (4), 2429-2437.
42. Cai, D.; Song, M. Preparation of fully exfoliated graphite oxide nanoplatelets in organic solvents. *J. Mater. Chem.* **2007**, *17* (35), 3678-3680.
43. Elaiwi, A.; Hitchcock, P. B.; Seddon, K. R.; Srinivasan, N.; Tan, Y.-M.; Welton, T.; Zora, J. A. Hydrogen bonding in imidazolium salts and its implications for ambient-temperature halogenoaluminate (III) ionic liquids. *J. Chem. Soc. Dalton Trans.* **1995**, (21), 3467-3472.
44. Fei, Z.; Zhao, D.; Geldbach, T. J.; Scopelliti, R.; Dyson, P. J. Brønsted acidic ionic liquids and their zwitterions: synthesis, characterization and pKa determination. *Chem. Eur. J.* **2004**, *10* (19), 4886-4893.
45. Yang, H.; Zhang, Q.; Shan, C.; Li, F.; Han, D.; Niu, L. Stable, conductive supramolecular composite of graphene sheets with conjugated polyelectrolyte. *Langmuir* **2010**, *26* (9), 6708-6712.
46. Zu, S.-Z.; Han, B.-H. Aqueous dispersion of graphene sheets stabilized by pluronic copolymers: formation of supramolecular hydrogel. *J. Phys. Chem. C* **2009**, *113* (31), 13651-13657.
47. Xu, J.; Wang, K.; Zu, S.-Z.; Han, B.-H.; Wei, Z. Hierarchical nanocomposites of polyaniline nanowire arrays on graphene oxide sheets with synergistic effect for energy storage. *ACS nano* **2010**, *4* (9), 5019-5026.
48. Chang, H.; Wang, G.; Yang, A.; Tao, X.; Liu, X.; Shen, Y.; Zheng, Z. A transparent, flexible, low - temperature, and solution - processible graphene composite electrode. *Adv. Funct. Mater.* **2010**, *20* (17), 2893-2902.
49. Allen, M. J.; Wang, M.; Jannuzzi, S. A.; Yang, Y.; Wang, K. L.; Kaner, R. B. Chemically induced folding of single and bilayer graphene. *Chem. Commun.* **2009**, (41), 6285-6287.
50. Chen, Y.; Zhang, X.; Yu, P.; Ma, Y. Stable dispersions of graphene and highly conducting graphene films: a new approach to creating colloids of graphene monolayers. *Chem. Commun.* **2009**, (30), 4527-4529.
51. Yang, Y.-K.; He, C.-E.; Peng, R.-G.; Baji, A.; Du, X.-S.; Huang, Y.-L.; Xie, X.-L.; Mai, Y.-W. Non-covalently modified graphene sheets by imidazolium ionic liquids for multifunctional polymer nanocomposites. *J. Mater. Chem.* **2012**, *22* (12), 5666-5675.
52. Kim, K. S.; Tarakeshwar, P.; Lee, J. Y. Molecular clusters of π -systems: theoretical studies of structures, spectra, and origin of interaction energies. *Chem. Rev.* **2000**, *100* (11), 4145-4186.

53. Yousuf, M.; Youn, I. S.; Yun, J.; Rasheed, L.; Valero, R.; Shi, G.; Kim, K. S. Violation of DNA neighbor exclusion principle in RNA recognition. *Chem. Sci.* **2016**, *7* (6), 3581-3588.
54. Seema, H.; Kemp, K. C.; Le, N. H.; Park, S.-W.; Chandra, V.; Lee, J. W.; Kim, K. S. Highly selective CO₂ capture by S-doped microporous carbon materials. *Carbon* **2014**, *66*, 320-326.

Table of Contents (TOC) Graphic

